

1 Modeling All Exceedances Above a Threshold Using an
2 Extremal Dependence Structure:
3 Inferences on Several Flood Characteristics

4 Mathieu Ribatet^{*,†} Taha B.M.J. Ouarda[†] Eric Sauquet^{*}
5 Jean-Michel Grésillon^{*}

6 Submitted to: *Water Resources Research*

7 ^{*} Cemagref Lyon, Unité de Recherche Hydrologie-Hydraulique, 3 bis quai Chauveau, CP220,
8 69336 Lyon cedex 09, France

9 [†] INRS-ETE, University of Québec, 490, de la Couronne Québec, Qc, G1K 9A9, CANADA.

10 Corresponding author: M. Ribatet; Email: ribatet@lyon.cemagref.fr
11 Phone: +33 4 72 20 87 64; Fax: +33 4 78 47 78 75

12 **Abstract**

13 Flood quantile estimation is of great importance for many engineering studies and policy deci-
14 sions. However, practitioners must often deal with small data available. Thus, the information
15 must be used optimally. In the last decades, to reduce the waste of data, inferential method-
16 ology has evolved from annual maxima modeling to peaks over a threshold one. To mitigate
17 the lack of data, peaks over a threshold are sometimes combined with additional information
18 - mostly regional and historical information. However, whatever the extra information is, the
19 most precious information for the practitioner is found at the target site. In this study, a model
20 that allows inferences on the whole time series is introduced. In particular, the proposed model
21 takes into account the dependence between successive extreme observations using an appropri-
22 ate extremal dependence structure. Results show that this model leads to more accurate flood
23 peak quantile estimates than conventional estimators. In addition, as the time dependence is
24 taken into account, inferences on other flood characteristics can be performed. An illustration
25 is given on flood duration. Our analysis shows that the accuracy of the proposed models to
26 estimate the flood duration is related to specific catchment characteristics. Some suggestions
27 to increase the flood duration predictions are introduced.

1 Introduction

Estimation of extreme flood events is an important stage for many engineering designs and risk management. This is a considerable task as the amount of data available is often small. Thus, to increase the precision and the quality of the estimates, several authors use extra information in addition to the target site one. For example, Ribatet et al. [2007a], Kjeldsen and Jones [2006, 2007] and Cunderlik and Ouarda [2006] add information from other homogeneous gaging stations. Werritty et al. [2006] and Reis Jr. and Stedinger [2005] use historical information to improve inferences. Incorporation of extra information in the estimation procedure is attractive but it should not be more prominent than the original data [Ribatet et al., 2007b]. Before looking at other kinds of information, it seems reasonable to use efficiently the one available at the target site. Most often, practitioners have initially the whole time series, not only the extreme observations. In particular, it is a considerable waste of information to reduce a time series to a sample of Annual Maxima (**AM**).

In this perspective, the Peaks Over Threshold (**POT**) approach is less wasteful as more than one event per year could be inferred. However, the declustering method used to identify independent events is quite subjective. Furthermore, even though a “quasi automatic” procedure was recently introduced by Ferro and Segers [2003], there is still a waste of information as only cluster maxima are used.

Coles et al. [1994] and Smith et al. [1997] propose an approach using Markov chain models that uses all exceedances and accounts for temporal dependence between successive observations. Finally, the entire information available within the time series is taken into account. More recently, Fawcett and Walshaw [2006] give an illustrative application of the Markov chain model to extreme wind speed modeling.

In this study, extreme flood events are of interest. The performance of the Markov chain model is compared to the conventional POT approach. The data analyzed consist of a collection of 50 French gaging stations. The area under study ranges from 2°W to 7°E and from 45°N to 51°N. The drainage areas vary from 72 to 38300 km² with a median value of 792 km². Daily observations were

55 recorded from 39 to 105 years, with a mean value of 60 years. For the remainder of this article, the
56 quantile benchmark values are derived from the maximum likelihood estimates on the whole times
57 series using a conventional POT analysis.

58 The paper is organized as follows. Section 2 introduces the theoretical aspects for the Markov
59 chain model, while Section 3 checks the relevance of the Markovian model hypothesis. Section 4
60 and 5 analyze the performance of the Markovian model to estimate the flood peaks and durations
61 respectively. Finally, some conclusions and perspectives are drawn in Section 6.

62 **2 A Markov Chain Model for Cluster Exceedances**

63 In this section, the extremal Markov chain model is presented. In the remainder of this article, it
64 is assumed that the flow Y_t at time t depends on the value Y_{t-1} at time $t - 1$. The dependence
65 between two consecutive observations is modeled by a first order Markov chain. Before introducing
66 the theoretical aspects of the model, it is worth justifying and describing the main advantages of
67 the proposed approach.

68 It is now well-known that the univariate Extreme Value Theory (**EVT**) is relevant when mod-
69 eling either AM or POT. Nevertheless, its extension to the multivariate case is surprisingly rarely
70 applied in practice. This work aims to motivate the use of the Multivariate EVT (**MEVT**). In
71 our application, the multivariate results are used to model the dependence between a set of lagged
72 values in a times series. Consequently, compared to the AM or the POT approaches, the amount
73 of observations used in the inference procedure is clearly larger. For instance, while only cluster
74 maxima are used in a POT analysis, all exceedances are inferred using a Markovian model.

75 **2.1 Likelihood function**

76 Let Y_1, \dots, Y_n be a stationary first-order Markov chain with a joint distribution function of two
77 consecutive observations $F(y_1, y_2)$, and $F(y)$ its marginal distribution. Thus, the likelihood function
78 L evaluated at points (y_1, \dots, y_n) is:

$$L(y_1, \dots, y_n) = f(y_1) \prod_{i=2}^n f(y_i | y_{i-1}) = \frac{\prod_{i=2}^n f(y_i, y_{i-1})}{\prod_{i=2}^{n-1} f(y_i)} \quad (1)$$

79 where $f(y_i)$ is the marginal density, $f(y_i | y_{i-1})$ is the conditional density, and $f(y_i, y_{i-1})$ is the joint
80 density of two consecutive observations.

81 To model all exceedances above a sufficiently large threshold u , the joint and marginal densities
82 must be known. Standard univariate EVT arguments [Coles, 2001] justify the use of a Generalized
83 Pareto Distribution (**GPD**) for $f(y_i)$ - e.g. a term of the denominator in equation (1). As a
84 consequence, the marginal distribution is defined by:

$$F(y) = 1 - \lambda \left(1 + \xi \frac{y - u}{\sigma} \right)_+^{-1/\xi}, \quad y \geq u \quad (2)$$

85 where $x_+ = \max(0, x)$, $\lambda = \Pr[Y \geq u]$, σ and ξ are the scale and shape parameters respectively.
86 Similarly, MEVT arguments [Resnick, 1987] argue for a bivariate extreme value distribution for
87 $f(y_i, y_{i-1})$ - e.g. a term of the numerator in equation (1). Thus, the joint distribution is defined
88 by:

$$F(y_1, y_2) = \exp[-V(z_1, z_2)], \quad y_1 \geq u, \quad y_2 \geq u \quad (3)$$

89 where V is a homogeneous function of order -1, e.g. $V(nz_1, nz_2) = n^{-1}V(z_1, z_2)$, satisfying
90 $V(z_1, \infty) = z_1^{-1}$ and $V(\infty, z_2) = z_2^{-1}$, and $z_i = -1/\log F(y_i)$, $i = 1, 2$.

91 Contrary to the univariate case, there is no finite parametrization for the V functions. Thus, it is
92 common to use specific parametric families for V such as the logistic [Gumbel, 1960], the asymmetric
93 logistic [Tawn, 1988], the negative logistic [Galambos, 1975] or the asymmetric negative logistic [Joe,
94 1990] models. Some details for these parametrisations are reported in Annex A. These models, as
95 all models of the form (3) are asymptotically dependent, that is [Coles et al., 1999]

$$\chi = \lim_{\omega \rightarrow 1} \chi(\omega) = \lim_{\omega \rightarrow 1} \Pr [F(Y_2) > \omega | F(Y_1) > \omega] > 0 \quad (4)$$

$$\bar{\chi} = \lim_{\omega \rightarrow 1} \bar{\chi}(\omega) = \lim_{\omega \rightarrow 1} \frac{2 \log(1-\omega)}{\log \Pr [F(Y_1) > \omega, F(Y_2) > \omega]} - 1 = 1 \quad (5)$$

96 Other parametric families exist to consider simultaneously asymptotically dependent and inde-
 97 pendent cases [Bortot and Tawn, 1998]. However, apart from a few particular cases (see Section 3),
 98 the data analyzed here seem to belong to the asymptotically dependent class. Consequently, in this
 99 work, only asymptotically dependent models are considered - i.e. of the form (1)–(3).

100 2.2 Inference

101 The Markov chain model is fitted using maximum censored likelihood estimation [Ledford and
 102 Tawn, 1996]. The contribution $L_n(y_1, y_2)$ of a point (y_1, y_2) to the numerator of equation (1) is
 103 given by:

$$L_n(y_1, y_2) = \begin{cases} \exp[-V(z_1, z_2)] [V_1(z_1, z_2)V_2(z_1, z_2) - V_{12}(z_1, z_2)] K_1 K_2, & \text{if } y_1 > u, y_2 > u \\ \exp[-V(z_1, z_2)] V_1(z_1, z_2) K_1, & \text{if } y_1 > u, y_2 \leq u \\ \exp[-V(z_1, z_2)] V_2(z_1, z_2) K_2, & \text{if } y_1 \leq u, y_2 > u \\ \exp[-V(z_1, z_2)], & \text{if } y_1 \leq u, y_2 \leq u \end{cases} \quad (6)$$

104 where $K_j = -\lambda_j \sigma^{-1} t_j^{1+\xi} z_j^2 \exp(1/z_j)$, $t_j = [1 + \xi(y_j - u)/\sigma]_+^{-1/\xi}$ and V_j, V_{12} are the partial derivative
 105 with respect to the component j and the mixed partial derivative respectively. The contribution
 106 $L_d(y_j)$ of a point y_j to the denominator of equation (1) is given by:

$$L_d(y_j) = \begin{cases} \sigma^{-1} \lambda [1 + \xi(y_j - u)/\sigma]_+^{-1/\xi - 1}, & \text{if } y_j > u, \\ 1 - \lambda, & \text{otherwise.} \end{cases} \quad (7)$$

107 Finally, the log-likelihood is given by:

$$\log L(y_1, \dots, y_n) = \sum_{i=2}^n \log L_n(y_{i-1}, y_i) - \sum_{i=2}^{n-1} \log L_d(y_i) \quad (8)$$

108 2.3 Return levels

109 Most often, the major issue of an extreme value analysis is the quantile estimation. As for the POT
 110 approach, return level estimates can be computed. However, as all exceedances are inferred, this
 111 is done in a different way as the dependence between successive observations must be taken into
 112 account. For a stationary sequence Y_1, Y_2, \dots, Y_n with a marginal distribution function F , Lindgren
 113 and Rootzen [1987] have shown that:

$$\Pr [\max \{Y_1, Y_2, \dots, Y_n\} \leq y] \approx F(y)^{n^\theta} \quad (9)$$

114 where $\theta \in [0, 1]$ is the extremal index and can be interpreted as the reciprocal of the mean cluster
 115 size [Leadbetter, 1983] - i.e. $\theta = 0.5$ means that extreme (enough) events are expected to occur by
 116 pair. $\theta = 1$ (resp. $\theta \rightarrow 0$) corresponds to the independent (resp. perfect dependent) case.

117 As a consequence, the quantile Q_T corresponding to the T -year return period is obtained by
 118 equating equation (9) to $1 - 1/T$ and solving for T . By definition, Q_T is the observation that is
 119 expected to be exceeded once every T years, i.e.,

$$Q_T = u - \sigma \xi^{-1} \left(1 - \left\{ \lambda^{-1} \left[1 - (1 - 1/T)^{1/(n^\theta)} \right] \right\}^{-\xi} \right) \quad (10)$$

120 It is worth emphasizing equation (9) as it has a large impact on both theoretical and practical
 121 aspects. Indeed, for the AM approach, equation (9) is replaced by

$$\Pr [\max \{Y_1, Y_2, \dots, Y_n\} \leq y] \approx G(y) \quad (11)$$

122 where G is the distribution function of the random variable $M_n = \max \{Y_1, Y_2, \dots, Y_n\}$, that is a
 123 generalized extreme value distribution. In particular, the equations (9) and (11) differ as the first

124 one is fitted to the whole observations Y_i , while the latter is fitted to the AM ones. By definition, the
 125 number n_Y of the Y_i observations is much larger than the size n_M of the AM data set. Especially,
 126 for daily data, $n_Y = 365n_M$.

127 [Figure 1 about here.]

128 From equation (10), the extremal index θ must be known to obtain quantile estimates. The
 129 methodology applied in this study is similar to the one suggested by Fawcett and Walshaw [2006].
 130 Once the Markovian model is fitted, 100 Markov chains of length 2000 were generated. For each
 131 chain, the extremal index is estimated using the estimator proposed by Ferro and Segers [2003] to
 132 avoid issues related to the choice of declustering parameter. In particular, the extremal index θ is
 133 estimated using the following equations:

$$\hat{\theta}(u) = \begin{cases} \max\left(1, \frac{2[\sum_{i=1}^{N-1}(T_i-1)]^2}{(N-1)\sum_{i=1}^{N-1}T_i^2}\right), & \text{if } \max\{T_i : 1 \leq i \leq N-1\} \leq 2 \\ \max\left(1, \frac{2(\sum_{i=1}^{N-1}T_i)^2}{(N-1)\sum_{i=1}^{N-1}(T_i-1)(T_i-2)}\right), & \text{otherwise} \end{cases} \quad (12)$$

134 where N is the number of observations exceeding the threshold u , T_i is the inter-exceedance time,
 135 e.g. $T_i = S_{i+1} - S_i$ and the S_i is the i -th exceedance time.

136 Lastly, the extremal index related to a fitted Markov chain model is estimated using the sample
 137 mean of the 100 extremal index estimations. Figure 1 represents the histogram of these 100 extremal
 138 index estimations. In this study, as lots of time series are involved, the number and length of the
 139 simulated Markov chains may be too small to lead to the most accurate extremal index estimations;
 140 but avoid intractable CPU times. If less sites are considered, it is preferable to increase these two
 141 values.

142 A preliminary study (not shown here) demonstrates that, for quantile estimation, this procedure
 143 was more accurate than estimating θ using the estimator of [Leadbetter, 1983]. This confirms the
 144 conclusions drawn by Fawcett [2005] for the extreme wind speed data.

145 3 Extreme Value Dependence Structure Assessment

146 Prior to performing any estimations, it is necessary to test whether: (a) the first order Markov
147 chain assumption and (b) the extreme value dependence structure (equation (3)) are appropriate
148 to model successive observations above the threshold u .

149 [Figure 2 about here.]

150 [Figure 3 about here.]

151 Figures 2 and 3 plot the auto-correlation functions and the scatter plots between two consecutive
152 observations for two different gaging stations. As the partial autocorrelation coefficient at lag 1
153 is large, Figure 2 and 3 (left panels) corroborate the (a) hypothesis. However, as some partial
154 auto-correlation coefficients are significant beyond lag 1, it may suggest that a higher-order model
155 may be more appropriate but does not necessarily mean that a first-order assumption is completely
156 flawed. Simplex plots [Coles and Tawn, 1991] (not shown) can be used to assess the suitability of
157 a second-order assumption over a first-order one. For our application, it seems that a first-order
158 model seems to be valid - except for the five slowest dynamic catchments.

159 Though it is an important stage because of its consequences on quantile estimates [Ledford
160 and Tawn, 1996; Bortot and Coles, 2000], verifying the (b) hypothesis is a considerable task. An
161 overwhelming dependence between consecutive observations at finite levels is not sufficient as it
162 does not give any information about the dependence relation at asymptotic levels. For instance,
163 the overwhelming dependence at lag 1 (Figure 2 and 3, right panels) does certainly not justify the
164 use of an asymptotic dependent model.

165 [Figure 4 about here.]

166 [Figure 5 about here.]

167 Figures 4 and 5 plot the evolution of the $\chi(\omega)$ and $\bar{\chi}(\omega)$ statistics as ω increases for two different
168 sites. For these figures, the confidence intervals are derived by bootstrapping contiguous blocks
169 to take into account the successive observations dependence [Ledford and Tawn, 2003]. The $\chi(\omega)$

170 and $\bar{\chi}(\omega)$ statistics seem to depict two different asymptotic extremal dependence. From Figure 4,
171 it seems that $\lim \chi(\omega) \gg 0$ and $\lim \bar{\chi}(\omega) = 1$ for $\omega \rightarrow 1$. On the contrary, Figure 5 advocates
172 for $\lim \chi(\omega) = 0$ and $\lim \bar{\chi}(\omega) < 1$ for $\omega \rightarrow 1$. Consequently, Figure 4 seems to conclude for an
173 asymptotic dependent case while Figure 5 for an asymptotic independent case.

174 In theory, asymptotic (in)dependence should not be assessed using scatterplots. However, these
175 two different features can be deduced from Figures 2 and 3. For Figure 2, the scatterplot (Y_{t-1}, Y_t)
176 is increasingly less spread as the observations becomes larger; while increasingly more spread for
177 Figure 3. In other words, for the first case, the dependence seems to become stronger at larger
178 levels while this is the contrary for the second case.

179 [Table 1 about here.]

180 [Figure 6 about here.]

181 Two specific cases for different asymptotic dependence structures were illustrated. Table 2 shows
182 the evolution of the $\chi(\omega)$ statistics as ω increases for all the sites under study. Most of the stations
183 have significantly positive $\chi(\omega)$ values. In addition, only 13 sites have a 95% confidence interval
184 that contains the 0 value. For 9 of these stations, the 95% confidence intervals correspond to the
185 theoretical lower and upper bounds; so that uncertainties are too large to determine the extremal
186 dependence class. For the $\bar{\chi}$ statistic, results are less clear-cut. Figure 6 represents the histograms
187 for $\bar{\chi}(\omega)$ for successive ω values. Despite only a few observations being close to 1, most of the
188 stations have a $\bar{\chi}(\omega)$ value greater than 0.75. These values can be considered as significantly high
189 as $-1 < \bar{\chi}(\omega) \leq 1$, for all ω . Consequently, models of the form (1)–(3) may be suited to model the
190 extremal dependence between successive observations.

191 Other methods exist to test the extremal dependence but were unconvincing for our application
192 [Ledford and Tawn, 2003; Falk and Michel, 2006]. Indeed, the approach of Falk and Michel [2006]
193 does not take into account the dependence between Y_{t-1} and Y_t ; while the test of Ledford and
194 Tawn [2003] appears to be poorly discriminatory for our case study.

195 **4 Performance of the Markovian Models on Quantile Esti-**
 196 **mation**

197 **4.1 Comparison between Markovian estimators**

198 In this section, the performance of six different extremal dependence structures is analyzed on the
 199 50 gaging stations introduced in section 1. These models are: *log* for the logistic, *nlog* for the
 200 negative logistic, *mix* for the mixed models and their relative asymmetric counterparts - e.g. *alog*,
 201 *anlog* and *amix*. To assess the impact of the dependence structure on flood peak estimation, the
 202 efficiency of each model to estimate quantiles with return periods 2, 10, 20, 50 and 100 years is
 203 evaluated.

204 As practitioners often have to deal with small record lengths in practice, the performance of the
 205 Markovian models is analyzed on all sub time series of length 5, 10, 15 and 20 years. Finally, to
 206 assess the efficiency for all the gaging stations considered in this study, the normalized bias (**nbias**),
 207 the variance (**var**) and the normalized mean squared error (**nmse**) are computed:

$$nbias = \frac{1}{N} \sum_{i=1}^N \frac{\hat{Q}_{i,T} - Q_T}{Q_T} \quad (13)$$

$$var = \frac{1}{N-1} \sum_{i=1}^N \left(\frac{\hat{Q}_{i,T} - Q_T}{Q_T} - nbias \right)^2 \quad (14)$$

$$nmse = \frac{1}{N} \sum_{i=1}^N \left(\frac{\hat{Q}_{i,T} - Q_T}{Q_T} \right)^2 \quad (15)$$

208 where Q_T is the benchmark T -year return level and $\hat{Q}_{i,T}$ is the i -th estimate of Q_T .

209 [Figure 7 about here.]

210 Figure 7 depicts the *nbias* densities for Q_{20} with a record length of 5 years. It is overwhelming
 211 that the extremal dependence structure has a great impact on the estimation of Q_{20} . Comparing
 212 the two panels, it can be noticed that the symmetric dependence structures give spreader densities;

213 that is, more variable estimates. Independently of the symmetry, Figure 7 shows that the mixed
214 dependence family is more accurate.

215 [Table 2 about here.]

216 Table 3 shows the *nbias*, *var* and *nmse* statistics for all the Markovian estimators as the record
217 length increases for quantile Q_{50} . This table confirms results derived from Figure 7. Indeed, the
218 asymmetric dependence structures give less variable and biased estimates - as their *nbias* and *var*
219 statistics are smaller. In addition, whatever the record length is, the Markovian models perform
220 with the same hierarchy; that is the *mix* and *amix* models are by far the most accurate estimators
221 - i.e. with the smallest *nmse* values. The same results (not shown) have been found for other
222 quantiles.

223 From an hydrological point of view, these two results are not surprising. The symmetric models
224 suppose that the variables Y_t and Y_{t+1} are exchangeable. In our context, exchangeability means
225 that the time series are reversible - e.g. the time vector direction has no importance. When dealing
226 with AM or POT and stationary time series, it is a reasonable hypothesis. For example, the MLE
227 remains the same with any permutations of the AM/POT sample. However, when modeling all
228 exceedances, the time direction can not be considered as reversible as flood hydrographs are clearly
229 non symmetric.

230 [Figure 8 about here.]

231 The Pickands' dependence function $A(\omega)$ [Pickands, 1981] is another representation for the
232 extremal dependence structure for any extreme value distribution. $A(\omega)$ is related to the V function
233 in equation (3) as follows:

$$A(\omega) = \frac{V(z_1, z_2)}{z_1^{-1} + z_2^{-1}}, \quad \omega = \frac{z_1}{z_1 + z_2} \quad (16)$$

234 Figure 8 represents the Pickands' dependence function for all the gaging stations and the three
235 asymmetric Markovian models. One major specificity of the mixed models is that these models can
236 not account for perfect dependence cases. In particular, the Pickands' dependence functions for

237 the mixed models satisfy $A(0.5) \geq 0.75$ while $A(0.5) \in [0.5, 1]$ for the logistic and negative logistic
238 models. From Figure 8, it can be seen that only few stations have a dependence function that could
239 not be modeled by the *amix* model. Therefore, the dependence range limitation of the *amix* model
240 does not seem too restrictive.

241 In this section, the effect of the extremal dependence structure has been assessed. It has been
242 established that the symmetric models are hydrologically inconsistent as they could not reproduce
243 the flood event asymmetry. In addition, for all the quantiles analyzed, the asymmetric mixed model
244 is the most accurate for flood peak estimations. Therefore, in the remainder of this section, only
245 the *amix* model will be compared to conventional POT estimators.

246 4.2 Comparison between *amix* and conventional POT estimators

247 In this section, the performance of the *amix* estimator is compared to the estimators usually used
248 in flood frequency analysis. For this purpose, the quantile estimates derived from the Maximum
249 Likelihood Estimator (**MLE**), the Unbiased and Biased Probability Weighted moments estimators
250 [Hosking and Wallis, 1987] (**PWU** and **PWB** respectively) are considered.

251 [Figure 9 about here.]

252 Figure 9 depicts the *nbias* densities for the *amix*, *MLE*, *PWU* and *PWB* estimators related
253 to the Q_5 , Q_{10} and Q_{20} estimations with a record length of 5 years. It can be seen that *amix* is the
254 most accurate model for all quantiles. Indeed, the *amix nbias* densities are the most sharp with a
255 mode close to 0. Focusing only on “classical” estimators (e.g. *MLE*, *PWU* and *PWB*), there is
256 no estimator that perform better than any other anytime. These two results advocate the use of
257 the *amix* model.

258 [Table 3 about here.]

259 Table 4 shows the performance of each estimator to estimate Q_{50} as the record length increases.
260 It can be seen that the *amix* model performs better than the conventional estimators for the whole
261 range of record lengths analyzed. First, *amix* has the same bias than the conventional estimators.

262 Thus, the *amix* dependence structure seems to be suited to estimate flood quantile estimates.
263 Second, because of its smaller variance, *amix* is more accurate than *MLE*, *PWU* and *PWB*
264 estimators. This smaller variance is mainly a result of all of the exceedances (not only cluster
265 maxima) being used in the inference procedure. Consequently, the *amix* model has a smaller *nmse*
266 - around half of the conventional models ones.

267 [Figure 10 about here.]

268 Figure 10 shows the evolution of the *nmse* as the return period increases for the *amix*, *MLE*,
269 *PWU* and *PWB* models. This figure corroborates the conclusions drawn from Figure 9 and Table 4.
270 It can be seen that the *amix* model has the smallest *nmse*, independently of the return period and
271 the record length. In addition, the *amix* becomes increasingly more efficient as the return period
272 increases - mostly for return periods greater than 20 years. While the conventional estimators
273 present an erratic *nmse* behavior as the return period increases, the *amix* model is the only one
274 that has a smooth evolution. To conclude, these results confirm that the *amix* model clearly
275 improves flood peak quantile estimates - especially for large return periods.

276 5 Inference on Other Flood Characteristics

277 As all exceedances are modeled using a first order Markov chain, it is possible to infer other quan-
278 tities than flood peaks - e.g. volume and duration. In this section, the ability of these Markovian
279 models to reproduce the flood duration is analyzed. For this purpose, the most severe flood hy-
280 drographs within each year are considered and normalized by their peak values. Consequently,
281 from this observed normalized hydrograph set, two flood characteristics derived from a data set of
282 hydrographs [Robson and Reed, 1999; Sauquet et al., 2008] are considered: (a) the duration d_{mean}
283 above 0.5 of the normalized hydrograph set mean and (b) the median d_{med} of the durations above
284 0.5 of each normalized hydrograph.

5.1 Global Performance

[Figure 11 about here.]

Figure 11 plots the flood durations d_{mean} and d_{med} biases derived from the three asymmetric Markovian models in function of their empirical estimates. It can be seen that no model leads to accurate flood duration estimations. In addition, the extremal dependence structure has a clear impact on these estimations. In particular, the *anlog* and *amix* models seem to underestimate the flood durations, while the *alog* model leads to overestimations. Consequently, two different conclusions can be drawn. First, as large durations are poorly estimated, higher order Markov chains may be of interest. However, this is a considerable task as higher dimensional multivariate extreme value distributions often lead to numerical problems. Instead of considering higher order, another alternative may be to change daily observations for d -day observations - where d is larger than 1. Second, it is overwhelming that the extremal dependence structure affects the flood duration estimations. As noticed in Section 2.1, there is no finite parametrization for the extremal dependence structure V - see Equation (3). Consequently, it seems reasonable to suppose that one suited for flood hydrograph estimation may exist.

[Figure 12 about here.]

Figure 12 depicts the observed normalized mean hydrographs and the ones predicted by the three asymmetric Markovian models. For the J0621610 station (left panel), the normalized hydrograph is well estimated by the three models; whereas for the L0400610 station (right panel), the normalized hydrograph is poorly predicted. This result confirms the inability of the three Markovian models to reproduce long flood events with daily data and a first order Markov chain.

[Figure 13 about here.]

Figure 13 represents the biases related to each value of the normalized mean hydrograph. In addition, to help estimator comparison, the *nmse* is reported at the right side. It can be seen that the *alog* model dramatically overestimates the hydrograph rising limb while giving reasonable estimations for the falling phase. The *anlog* model slightly overestimates the rising part while

311 strongly underestimates the falling one. The *amix* model always leads to underestimations - this
 312 is more pronounced for the falling limb. However, despite these different behaviors, these three
 313 estimators seems to have a similar performance - in terms of *nmse*.

314 [Figure 14 about here.]

315 Figure 14 represents the spatial distribution of the *nmse* on the normalized mean hydrograph
 316 estimation for each Markovian model. It seems that there is a specific spatial distribution. In
 317 particular, the worst cases are related to the middle part of France. In addition, for different
 318 extremal dependence structures, the best *nmse* values correspond to different spatial locations.
 319 The *alog* model is more accurate for the extreme north part of France; the *anlog* model is more
 320 efficient for the east part of France; while the *amix* model performs best in the middle part of
 321 France. Consequently, as at a global scale no model is accurate to estimate the normalized mean
 322 hydrograph, it is worth trying to identify which catchment types are related to the best estimations.

323 For our data set, this is a considerable task. No standard statistical technique lead to reasonable
 324 results. In particular, the principal component analysis, hierarchical classification, sliced inverse
 325 regression lead to no conclusion about which catchment types are more suitable for our models.
 326 Only a regression approach gives some first guidelines. For this purpose, a regression between the
 327 *nbias* on the d_{mean} estimation for each asymmetric model and some geomorphologic and hydrologic
 328 indices are performed. The effect of the drainage area, an index of catchment slope derived from
 329 the hypsometric curve [Roche, 1963], the Base Flow Index (**BFI**) [Tallaksen and Van Lanen, 2004,
 330 Section 5.3.3] and an index characterizing the rainfall persistence [Vaskova and Francès, 1998] are
 331 considered.

$$nbias(d_{mean}; analog) = 0.89 - 2.19BFI, \quad R^2 = 0.40 \quad (17)$$

$$nbias(d_{mean}; amix) = 0.49 - 1.74BFI, \quad R^2 = 0.43 \quad (18)$$

332 From equations (17) and (18), the *BFI* variable explains around 40% of the variance. Despite
 333 the fact that a large variance proportion is not taken into account, the *BFI* is clearly related to the

334 d_{mean} estimation performance. These equations indicate that the *anlog* (resp. *amix*) model is more
335 accurate to reproduce the d_{mean} variable for gaging stations with a *BFI* around 0.4 (resp. 0.28).
336 These *BFI* values correspond to catchments with moderate up to flash flow regimes respectively.
337 These results corroborate the ones derived from Figure 13: the first order Markovian models with a
338 1-day lag conditioning are not appropriate for long flood duration estimations. Consequently, while
339 no physiographic characteristic is related to the *alog* performance; it is suggested, for such 1-day
340 lag conditioning, to use the *anlog* and *amix* models for quick basins.

341 6 Conclusion

342 Despite that univariate EVT is widely applied in environmental sciences, its multivariate extension
343 is rarely considered. This work tries to promote the use of the MEVT in hydrology. In this work, the
344 bivariate case was considered as the dependence between two successive observations was modeled
345 using a first order Markov chain. This approach has two main advantages for practitioners as: (a)
346 the number of data to be inferred increases considerably and (b) other features can be estimated -
347 flood duration, volume.

348 In this study, a comparison between six different extremal dependence structures (including
349 both symmetric and asymmetric forms) has been performed. Results show that an asymmetric
350 dependence structure is more relevant. From a hydrological point of view, this asymmetry is
351 rational as flood hydrographs are asymmetric. In particular, for our data, the asymmetric mixed
352 model gives the most accurate flood peak estimations and clearly improves flood peak estimations
353 compared to conventional estimators independently of the return period considered.

354 The ability of these Markovian models to estimate the flood duration was carried out. It has
355 been shown that, at first sight, no dependence structure is able to reproduce the flood hydrograph
356 accurately. However, it seems that the *anlog* and *amix* models may be more appropriate when
357 dealing with moderate up to flash flow regimes. These results depend strongly on the conditioning
358 term (i.e. $\Pr[Y_t \leq y_t | Y_{t-\delta} = y_{t-\delta}]$) of the first order Markov chain and on the auto-correlation
359 within the time series. In our application, $\delta = 1$ and daily time step was considered.

360 More general conclusions can be drawn. The weakness of the proposed models to derive consis-
361 tent flood hydrographs may not be related to the daily time step but to the inadequacy between the
362 conditioning term and the flood dynamics. To ensure better results, higher order Markov chains
363 may be of interest [Fawcett and Walshaw, 2006]. However, as numerical problems may arise, an-
364 other alternative may be to still consider a first order chain but to change the “conditioning lag
365 value” δ . In particular, for some basins, it may be more relevant to condition the Markov chain
366 with a larger but more appropriate lag value.

367 Another option to improve the proposed models for flood hydrograph estimation is to use a more
368 suitable dependence function V . As there is no finite parametrization for the extremal dependence
369 structure, it seems reasonable that one more appropriate for flood hydrographs may exist. In this
370 work, results show that the *anlog* model is more able to reproduce the hydrograph rising part, while
371 the *alog* is better for the falling phase. Define

$$V(z_1, z_2) = \alpha V_1(z_1, z_2) + \beta V_2(z_1, z_2)$$

372 where V_1 (resp. V_2) is the extremal dependence function for the *alog* (resp. *anlog*) model and α and
373 β are real constants such as $\alpha + \beta = 1$. By definition, V is a new extremal dependence function.
374 In particular, V may combine the accuracy of the *alog* and *anlog* models for both the rising
375 and falling part of the flood hydrograph. Another alternative may be to look at non-parametric
376 Pickands’ dependence function estimators [Capéraà et al., 1997] but that will require techniques to
377 simulate Markov chains from these non-parametric estimations.

378 All statistical analysis were performed within the R Development Core Team [2007] framework.
379 In particular, the POT package [Ribatet, 2007] integrates the tools that were developed to carry out
380 the modeling effort presented in this paper. This package is available, free of charge, at the website
381 <http://www.R-project.org>, section CRAN, Packages or at its own webpage <http://pot.r-forge.r-project.org/>.

382 **Acknowledgments**

383 The authors wish to thank the French HYDRO database for providing the data. Benjamin Renard
384 is acknowledged for criticizing thoroughly the data analyzed in this study.

385 **A Parametrization for the Extremal Dependence**

386 This annex presents some useful results for the six extremal dependence models that have been
387 considered in this work. As first order Markov chains were used, only the bivariate results are
388 described.

389 [Table 4 about here.]

Table 1: Partial and mixed partial derivatives, definition domain, total independent and perfect dependent cases for each extremal asymmetric dependence function V .

Model	Asymmetric Models		
	<i>alog</i>	<i>anlog</i>	<i>amlog</i>
$V(x, y)$	$\frac{1-\theta_1}{x} + \frac{1-\theta_2}{y} + \left[\left(\frac{x}{\theta_1} \right)^{-1/\alpha} + \left(\frac{y}{\theta_2} \right)^{-1/\alpha} \right]^\alpha$	$\frac{1}{x} + \frac{1}{y} - \left[\left(\frac{x}{\theta_1} \right)^\alpha + \left(\frac{y}{\theta_2} \right)^\alpha \right]^{-1/\alpha}$	$\frac{1}{x} + \frac{1}{y} - \frac{(2\alpha+1)}{(x+y)^\alpha}$
$V_1(x, y)$	$-\frac{1-\theta_1}{x^2} - \theta_1^{\frac{1}{\alpha}} x^{-\frac{1}{\alpha}-1} \left[\left(\frac{x}{\theta_1} \right)^{-1/\alpha} + \left(\frac{y}{\theta_2} \right)^{-1/\alpha} \right]^{\alpha-1}$	$-\frac{1}{x^2} + \theta_1^{-\alpha} x^{\alpha-1} \left[\left(\frac{x}{\theta_1} \right)^\alpha + \left(\frac{y}{\theta_2} \right)^\alpha \right]^{-1/\alpha-1}$	$-\frac{1}{x^2} - \frac{2\alpha+\theta}{(x+y)^2} + \frac{\theta}{(x+y)^\alpha}$
$V_2(x, y)$	$-\frac{1-\theta_2}{y^2} - \theta_2^{\frac{1}{\alpha}} y^{-\frac{1}{\alpha}-1} \left[\left(\frac{x}{\theta_1} \right)^{-1/\alpha} + \left(\frac{y}{\theta_2} \right)^{-1/\alpha} \right]^{\alpha-1}$	$-\frac{1}{y^2} + \theta_2^{-\alpha} y^{\alpha-1} \left[\left(\frac{x}{\theta_1} \right)^\alpha + \left(\frac{y}{\theta_2} \right)^\alpha \right]^{-1/\alpha-1}$	$-\frac{1}{y^2} - \frac{\alpha+\theta}{(x+y)^2} + \frac{\theta}{(x+y)^\alpha}$
$V_{12}(x, y)$	$\frac{\alpha-1}{\alpha} (\theta_1 \theta_2)^{\frac{1}{\alpha}} (xy)^{-\frac{1}{\alpha}-1} \left[\left(\frac{x}{\theta_1} \right)^{-1/\alpha} + \left(\frac{y}{\theta_2} \right)^{-1/\alpha} \right]^{\alpha-2}$	$-(\alpha+1)(\theta_1 \theta_2)^{-\alpha} (xy)^{\alpha-1} \left[\left(\frac{x}{\theta_1} \right)^\alpha + \left(\frac{y}{\theta_2} \right)^\alpha \right]^{-1/\alpha-2}$	$\frac{6\alpha+4\theta}{(x+y)^3} - 6\frac{\theta}{(x+y)^\alpha}$
$A(w)$	$(1-\theta_1)(1-w) + (1-\theta_2)w + \left[(1-w)^{\frac{1}{\alpha}} \theta_1^{\frac{1}{\alpha}} + w^{\frac{1}{\alpha}} \theta_2^{\frac{1}{\alpha}} \right]^\alpha$	$1 - \left[\left(\frac{1-w}{\theta_1} \right)^{-\alpha} + \left(\frac{w}{\theta_2} \right)^{-\alpha} \right]^{-\frac{1}{\alpha}}$	$\theta w^3 + \alpha w^2 - \frac{\theta}{(x+y)^\alpha}$
Independence	$\alpha = 1$ or $\theta_1 = 0$ or $\theta_2 = 0$	$\alpha \rightarrow 1$ or $\theta_1 \rightarrow 0$ or $\theta_2 \rightarrow 0$	$\alpha = 0$
Total dependence	$\alpha \rightarrow 0$	$\alpha \rightarrow +\infty$	Never
Constraint	$0 < \alpha \leq 1, 0 \leq \theta_1, \theta_2 \leq 1$	$\alpha > 0, 0 < \theta_1, \theta_2 \leq 1$	$\alpha \geq 0, \alpha + 2\theta \leq 1$

References

- 390
391 P. Bortot and S. Coles. The multivariate Gaussian tail model: An application to oceanographic
392 data. *Journal of the Royal Statistical Society. Series C: Applied Statistics*, 49(1):31–49, 2000.
- 393 P. Bortot and J.A. Tawn. Models for the extremes of Markov chains. *Biometrika*, 85(4):851–867,
394 1998. ISSN 00063444.
- 395 P. Capéraà, A.-L. Fougères, and C. Genest. A nonparametric estimation procedure for bivariate
396 extreme value copulas. *Biometrika*, 84(3):567–577, 1997. ISSN 00063444.
- 397 S. Coles. *An Introduction to Statistical Modelling of Extreme Values*. Springer Series in Statistics.
398 Springer Series in Statistics, London, 2001.
- 399 S. Coles and J.A. Tawn. Modelling Extreme Multivariate Events. *Journal of the Royal Statistical*
400 *Society. Series B (Methodological)*, 53(2):377–392, 1991. ISSN 0035-9246.
- 401 S. Coles, J.A. Tawn, and R.L. Smith. A seasonal Markov model for extremely low temperature.
402 *Environmetrics*, 5:221–239, 1994.
- 403 S. Coles, J. Heffernan, and J.A. Tawn. Dependence Measures for Extreme Value Analyses. *Extremes*,
404 2(4):339–365, December 1999.
- 405 J.M. Cunderlik and T.B.M.J. Ouarda. Regional flood-duration-frequency modeling in the changing
406 environment. *Journal of Hydrology*, 318(1-4):276–291, 2006.
- 407 M. Falk and R. Michel. Testing for tail independence in extreme value models. *Annal. Inst. Stat.*
408 *Math.*, 58(2):261–290, 2006. ISSN 00203157.
- 409 L. Fawcett. *Statistical Methodology for the Estimation of Environmental Extremes*. PhD thesis,
410 University of Newcastle upon Tyne, 2005.
- 411 L. Fawcett and D. Walshaw. Markov chain models for extreme wind speeds. *Environmetrics*, 17
412 (8):795–809, 2006. ISSN 11804009.
- 413 C.A.T. Ferro and J. Segers. Inference for clusters of extreme values. *Journal of the Royal Statistical*
414 *Society. Series B: Statistical Methodology*, 65(2):545–556, 2003. ISSN 13697412.
- 415 J. Galambos. Order statistics of samples from multivariate distributions. *Journal of the American*
416 *Statistical Association*, 9:674–680, 1975.
- 417 E.J. Gumbel. Bivariate exponential distributions. *Journal of the American Statistical Association*,
418 55(292):698–707, 1960.
- 419 J.R.M. Hosking and J.R. Wallis. Parameter and Quantile Estimation for the Generalized Pareto
420 Distribution. *Technometrics*, 29(3):339–349, 1987.
- 421 H. Joe. Families of min-stable multivariate exponential and multivariate extreme value distributions.
422 *Statist. Probab. Lett.*, 9:75–82, 1990.
- 423 T.R. Kjeldsen and D. Jones. Estimation of an index flood using data transfer in the UK. *Hydrol.*
424 *Sci. J.*, 52(1):86–98, 2007. ISSN 02626667.

- 425 T.R. Kjeldsen and D.A. Jones. Prediction uncertainty in a median-based index flood method using
426 L moments. *Water Resources Research*, 42(7):–, 2006. ISSN 00431397.
- 427 M.R. Leadbetter. Extremes and local dependence in stationary sequences. *Probability Theory and
428 Related Fields (Historical Archive)*, 65(2):291–306, 1983.
- 429 A.W. Ledford and J.A. Tawn. Statistics for near independence in multivariate extreme values.
430 *Biometrika*, 83:169–187, 1996.
- 431 A.W. Ledford and J.A. Tawn. Diagnostics for dependence within time series extremes. *Journal of
432 the Royal Statistical Society. Series B: Statistical Methodology*, 65(2):521–543, 2003.
- 433 G. Lindgren and H. Rootzen. Extreme values: theory and technical applications. *Scandinavian
434 journal of statistics*, 14(4):241–279, 1987.
- 435 J. Pickands. Multivariate Extreme Value Distributions. In *Proceedings 43rd Session International
436 Statistical Institute*, 1981.
- 437 R Development Core Team. *R: A Language and Environment for Statistical Computing*. R Founda-
438 tion for Statistical Computing, Vienna, Austria, 2007. URL <http://www.R-project.org>. ISBN
439 3-900051-07-0.
- 440 D.S. Reis Jr. and J.R. Stedinger. Bayesian MCMC flood frequency analysis with historical infor-
441 mation. *Journal of Hydrology*, 313(1-2):97–116, 2005. ISSN 00221694.
- 442 S.I. Resnick. *Extreme Values, Regular Variation and Point Processes*. New–York: Springer–Verlag,
443 1987.
- 444 M. Ribatet. POT: Modelling Peaks Over a Threshold. *R News*, 7(1):34–36, April 2007.
- 445 M. Ribatet, E. Sauquet, J.-M. Grésillon, and T.B.M.J. Ouarda. A regional Bayesian POT model
446 for flood frequency analysis. *Stochastic Environmental Research and Risk Assessment (SERRA)*,
447 21(4):327–339, 2007a.
- 448 M. Ribatet, E. Sauquet, J.-M. Grésillon, and T.B.M.J. Ouarda. Usefulness of the Reversible Jump
449 Markov Chain Monte Carlo Model in Regional Flood Frequency Analysis. *Water Resources
450 Research*, 43(8):W08403, 2007b. doi: 10.1029/2006WR005525.
- 451 A.J. Robson and D.W. Reed. *Flood Estimation Handbook*, volume 3. Institute of Hydrology,
452 Wallingford, 1999.
- 453 M. Roche. *Hydrologie de surface*. Gauthier-Villars, Paris, 1963.
- 454 E. Sauquet, M.-H. Ramos, L. Chapel, and P. Bernardara. Stream flow scaling properties: investigat-
455 ing characteristic scales from different statistical approaches. *Accepted in Hydrological Processes*,
456 2008. doi: 10.1002/hyp.6952.
- 457 R.L. Smith, J.A. Tawn, and S.G. Coles. Markov chain models for threshold exceedances. *Biometrika*,
458 84(2):249–268, 1997. ISSN 00063444.
- 459 L. Tallaksen and H. Van Lanen. *Hydrological Drought: Processes and Estimation Methods for
460 Streamflow and Groundwater*, volume 48. Elsevier, 2004.

- 461 J.A. Tawn. Bivariate extreme value theory: Models and estimation. *Biometrika*, 75(3):397–415,
462 1988.
- 463 I. Vaskova and F. Francès. Rainfall analysis and regionalization computing intensity-duration-
464 frequency curves. In *Flood Aware Final Report*, pages 95–108. Cemagref edition, 1998.
- 465 A. Werritty, J.L. Paine, N. Macdonald, J.S. Rowan, and L.J. McEwen. Use of multi-proxy flood
466 records to improve estimates of flood risk: Lower River Tay, Scotland. *Catena*, 66(1-2):107–119,
467 2006. ISSN 03418162.

468 **List of Figures**

469 1 Histogram of the extremal index estimations from the 100 simulated Markov Chains
470 of length 2000. 24
471 2 Autocorrelation plot (left panel) and scatterplot of the time series at lag 1 (right
472 panel) for the Somme river at Abbeville (E6470910). 25
473 3 Autocorrelation plot (left panel) and scatterplot of the time series at lag 1 (right
474 panel) for the Moselle river at Noircieux (A4200630). 26
475 4 Plot of the χ and $\bar{\chi}$ statistics and the related 95% confidence intervals for the Somme
476 river at Abbeville (E6470910). The solid blue lines are the theoretical bounds. . . . 27
477 5 Plot of the χ and $\bar{\chi}$ statistics and the related 95% intervals for the Moselle river at
478 Noircieux (A4200630). The solid blue lines are the theoretical bounds. 28
479 6 Histograms of the $\bar{\chi}(\omega)$ statistics for different ω values. Left panel: $\omega = 0.98$, middle
480 panel: $\omega = 0.985$ and right panel: $\omega = 0.99$ 29
481 7 Densities of the normalized biases of Q_{20} estimates for the symmetric Markovian
482 models (left panel) and the asymmetric ones (right panel). Target site record length:
483 5 years. 30
484 8 Representation of the Pickands' dependence functions for the 50 gaging stations.
485 Left panel : *alog*, middle panel: *anlog* and right panel: *amix*. "+" represents the
486 theoretical dependence bound for the *amix* model. 31
487 9 Densities of the normalized biases for the *amix* model and the *MLE*, *PWU*, and
488 *PWB* estimators for quantiles Q_5 (left panel), Q_{10} (middle panel) and Q_{20} (right
489 panel). Record length: 5 years. 32
490 10 Evolution of the *nmse* as the return period increases for the *amix*, *MLE*, *PWU* and
491 *PWB* estimators. Record length: (a) 5 years, (b) 10 years, (c) 15 years and (d) 20
492 years. 33
493 11 d_{mean} and d_{med} normalized biases in function of the theoretical values for the three
494 asymmetric Markovian models. 34
495 12 Observed and simulated normalized mean hydrographs for the J0621610 (left panel)
496 and the L0400610 (right panel) stations. 35
497 13 Evolution of the biases for the normalized mean hydrograph estimations in function
498 of the distance of the flood peak time. 36
499 14 *nmse* spatial distribution according for the three Markovian models. Left panel:
500 *alog*, middle panel: *anlog* and right panel: *amix*. The radius is proportional to the
501 *nmse* value. 37

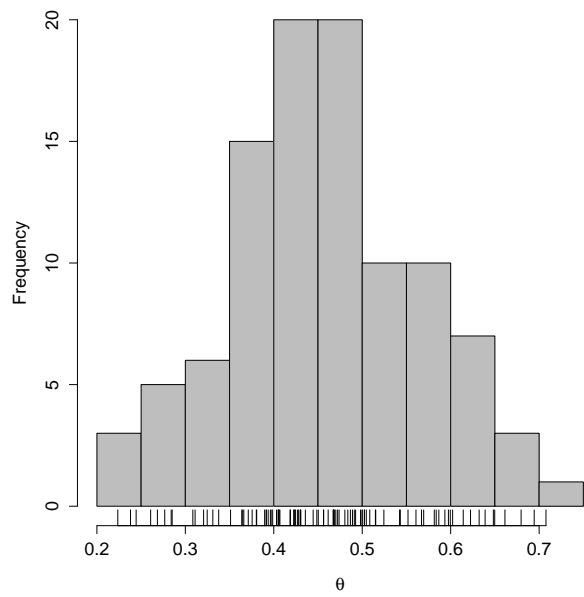


Figure 1: Histogram of the extremal index estimations from the 100 simulated Markov Chains of length 2000.

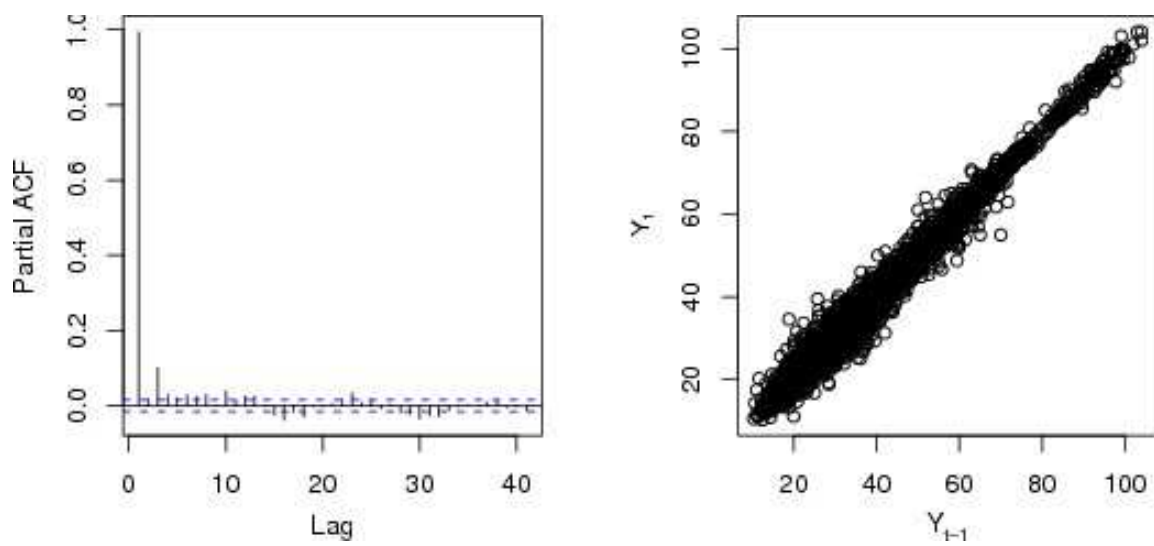


Figure 2: Autocorrelation plot (left panel) and scatterplot of the time series at lag 1 (right panel) for the Somme river at Abbeville (E6470910).

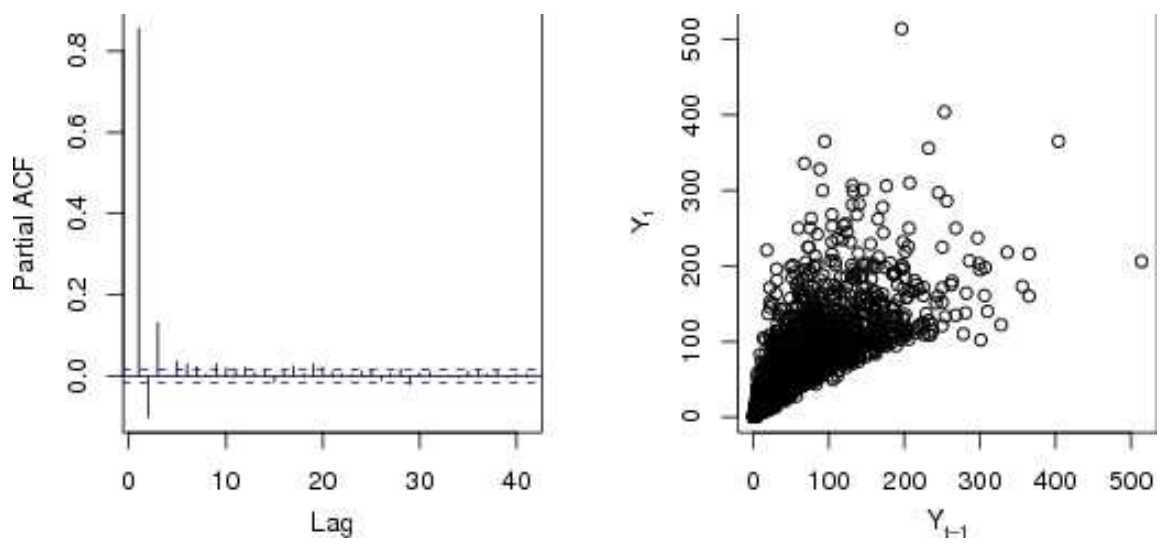


Figure 3: Autocorrelation plot (left panel) and scatterplot of the time series at lag 1 (right panel) for the Moselle river at Noirgueux (A4200630).

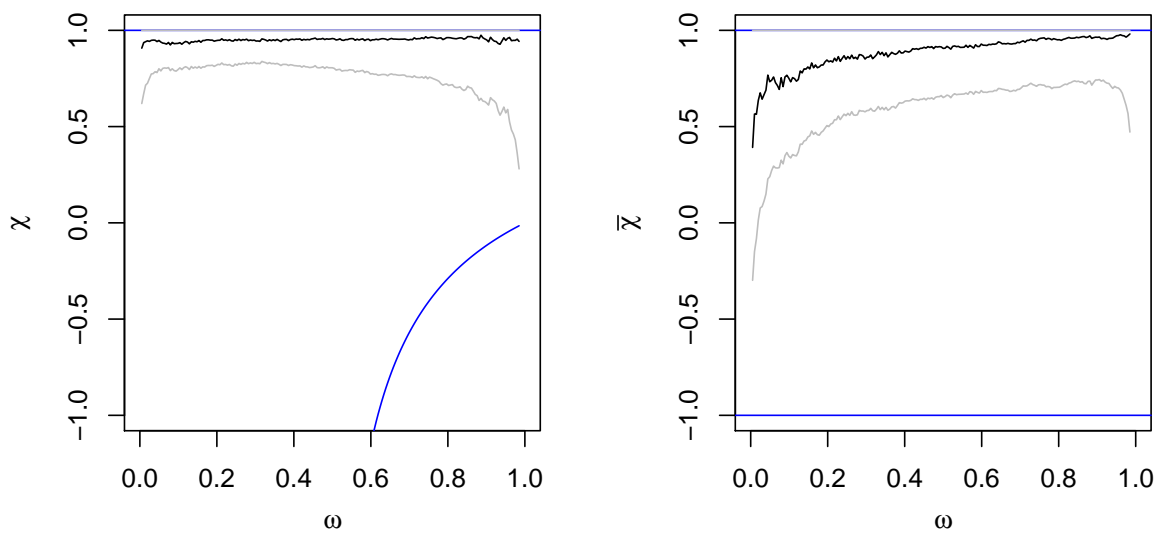


Figure 4: Plot of the χ and $\bar{\chi}$ statistics and the related 95% confidence intervals for the Somme river at Abbeville (E6470910). The solid blue lines are the theoretical bounds.

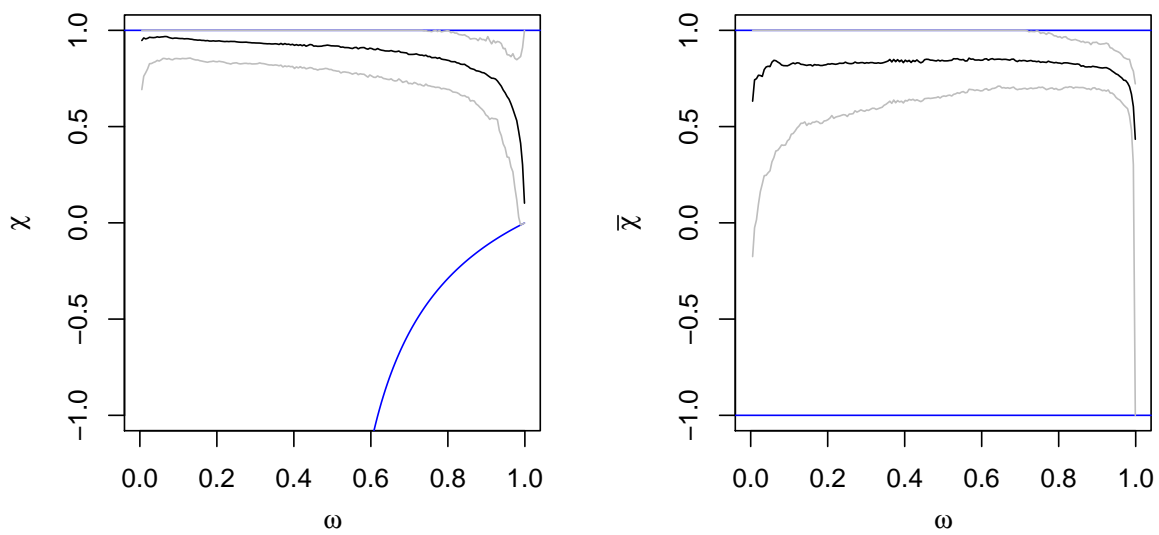


Figure 5: Plot of the χ and $\bar{\chi}$ statistics and the related 95% intervals for the Moselle river at Noirgueux (A4200630). The solid blue lines are the theoretical bounds.

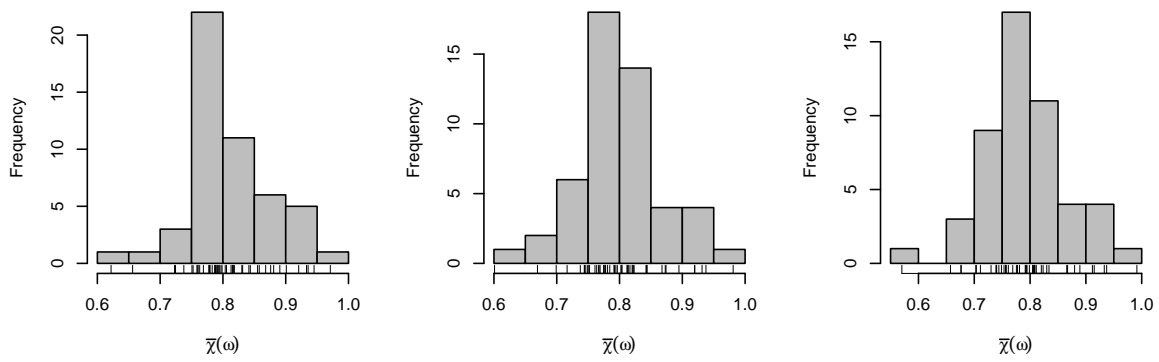


Figure 6: Histograms of the $\bar{\chi}(\omega)$ statistics for different ω values. Left panel: $\omega = 0.98$, middle panel: $\omega = 0.985$ and right panel: $\omega = 0.99$.

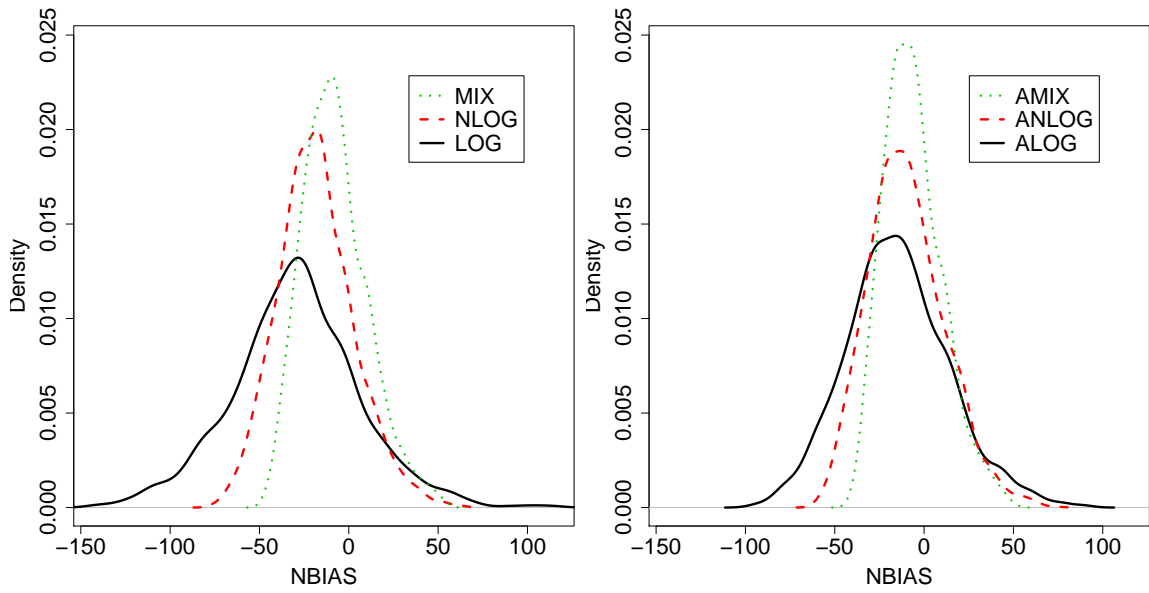


Figure 7: Densities of the normalized biases of Q_{20} estimates for the symmetric Markovian models (left panel) and the asymmetric ones (right panel). Target site record length: 5 years.

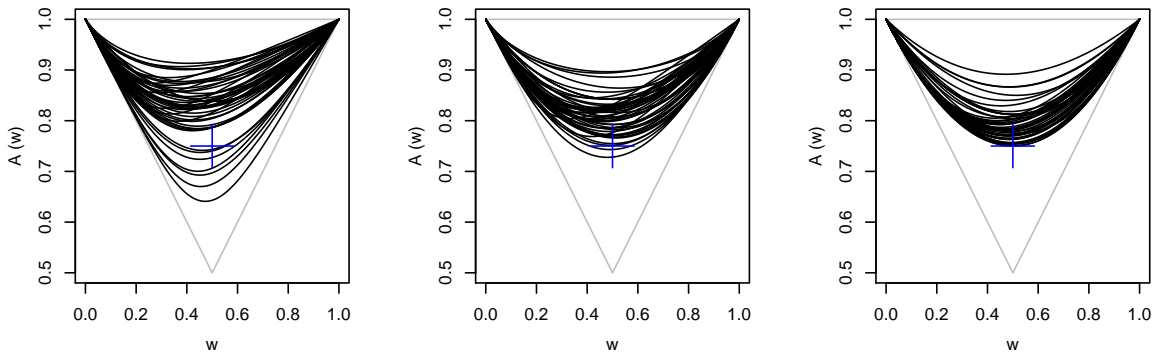


Figure 8: Representation of the Pickands' dependence functions for the 50 gaging stations. Left panel : *alog*, middle panel: *anlog* and right panel: *amix*. “+” represents the theoretical dependence bound for the *amix* model.

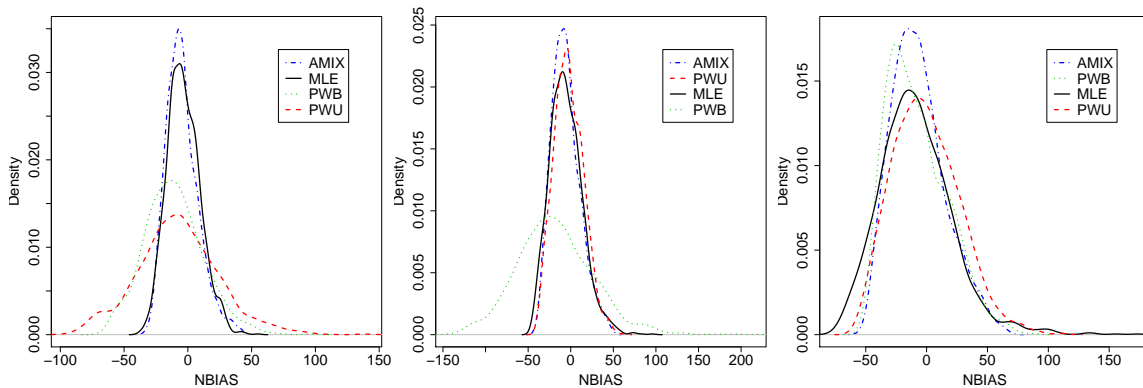


Figure 9: Densities of the normalized biases for the *amix* model and the *MLE*, *PWU*, and *PWB* estimators for quantiles Q_5 (left panel), Q_{10} (middle panel) and Q_{20} (right panel). Record length: 5 years.

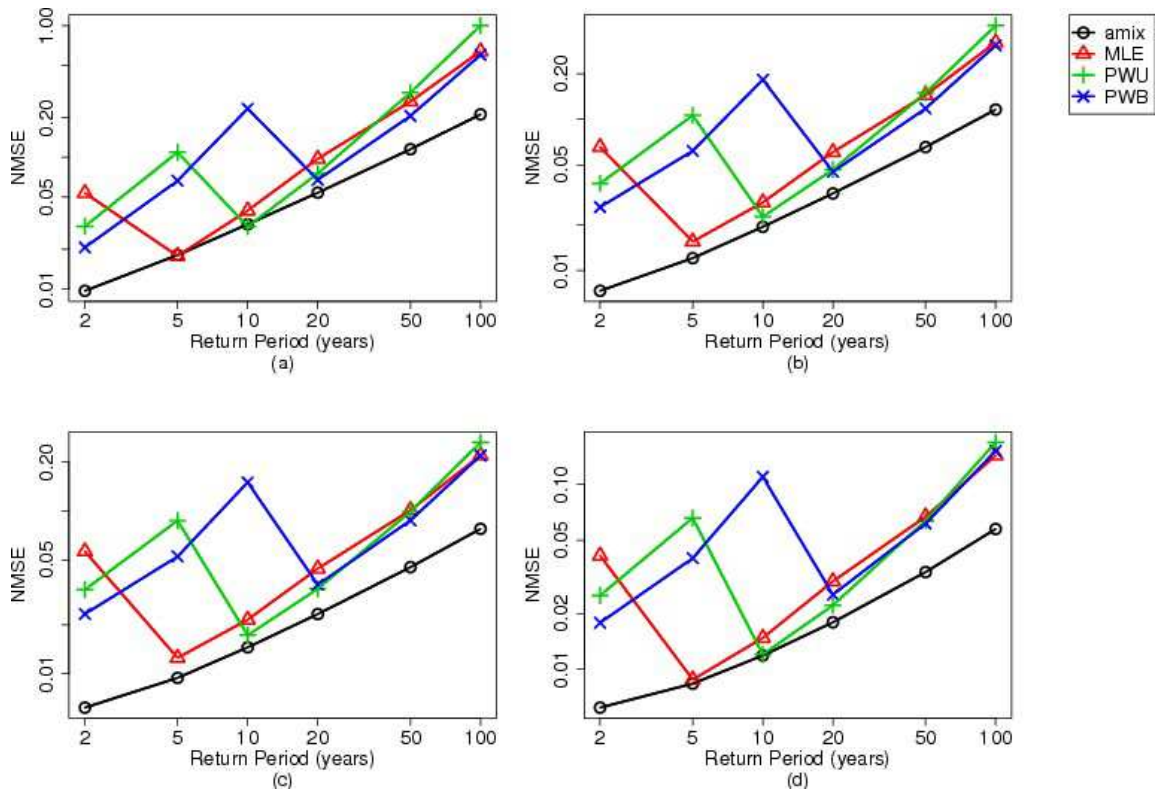


Figure 10: Evolution of the $nmse$ as the return period increases for the *amix*, *MLE*, *PWU* and *PWB* estimators. Record length: (a) 5 years, (b) 10 years, (c) 15 years and (d) 20 years.

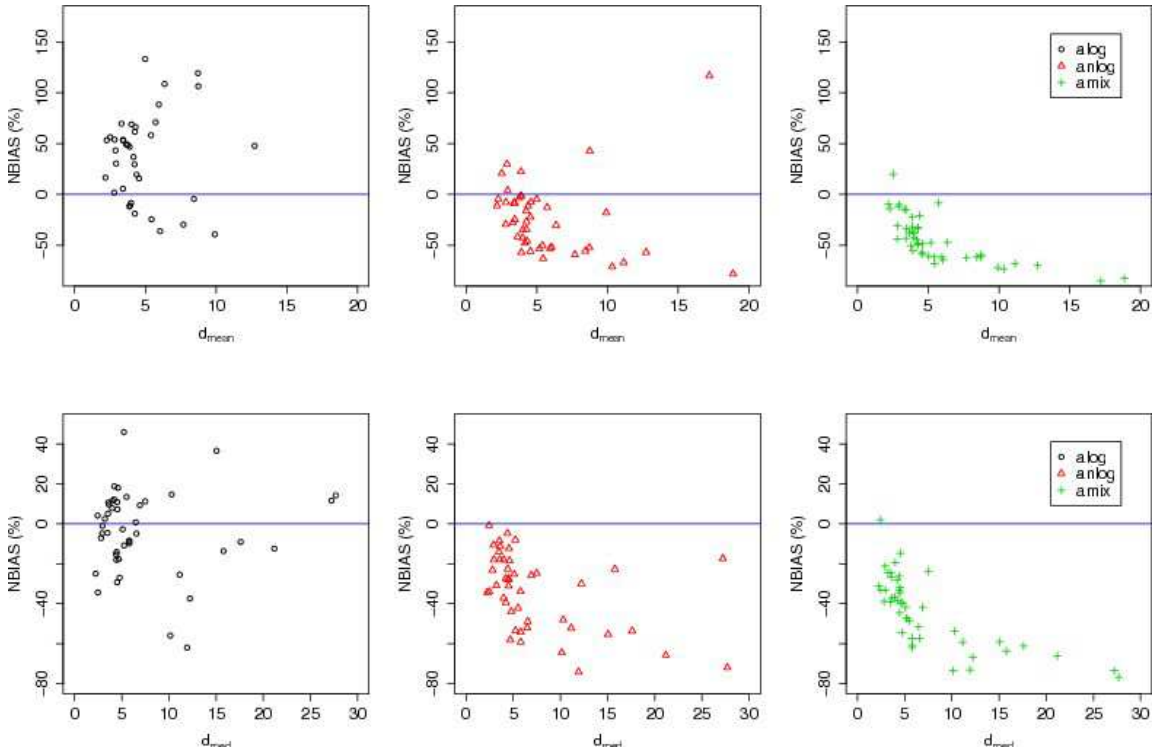


Figure 11: d_{mean} and d_{med} normalized biases in function of the theoretical values for the three asymmetric Markovian models.

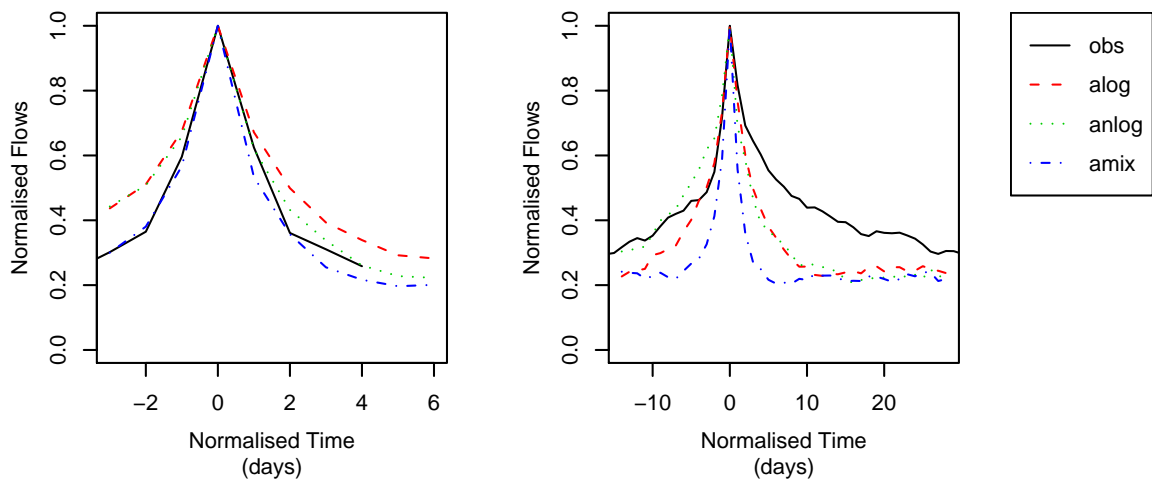


Figure 12: Observed and simulated normalized mean hydrographs for the J0621610 (left panel) and the L0400610 (right panel) stations.

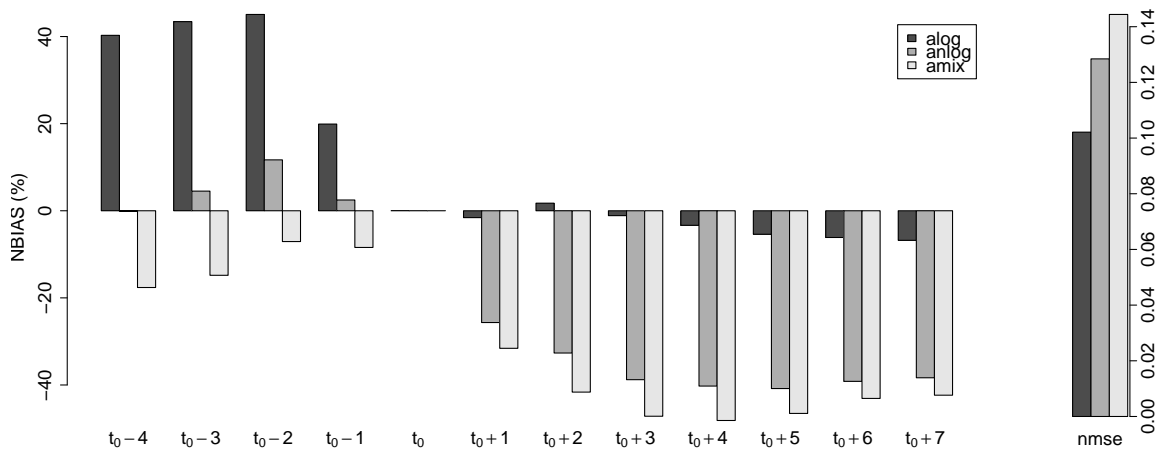


Figure 13: Evolution of the biases for the normalized mean hydrograph estimations in function of the distance of the flood peak time.

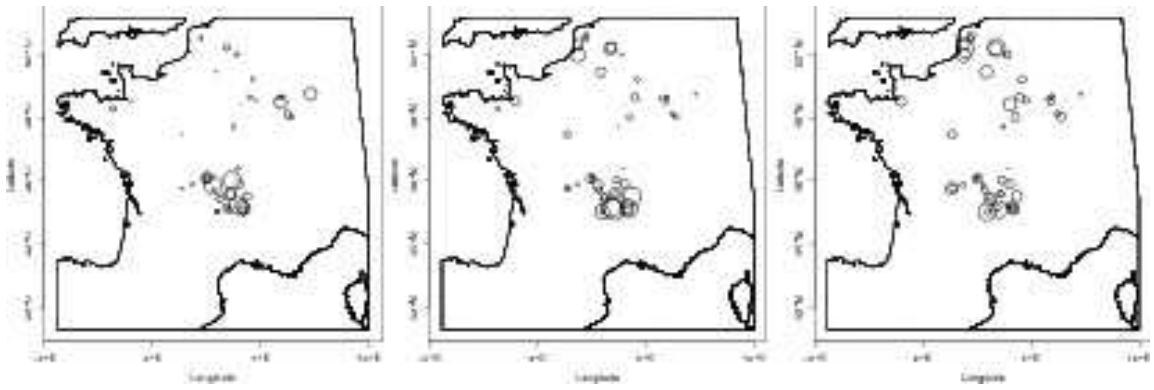


Figure 14: $nmse$ spatial distribution according for the three Markovian models. Left panel: *alog*, middle panel: *anlog* and right panel: *amix*. The radius is proportional to the $nmse$ value.

502 **List of Tables**

503	1	Partial and mixed partial derivatives, definition domain, total independent and perfect dependent cases for each extremal asymmetric dependence function V	19
504			
505	2	$\chi(\omega)$ statistics for all stations. $\omega = 0.98, 0.985, 0.99$	39
506	3	Several characteristics of the Markovian estimators on Q_{50} estimation as the record length increases. Standard errors are reported in brackets.	40
507			
508	4	Several characteristics of the <i>amix</i> , <i>MLE</i> , <i>PWU</i> and <i>PWB</i> estimators for Q_{50} estimation as the record length increases. Standard errors are reported in brackets. .	41
509			
510	5	Partial and mixed partial derivatives, definition domain, total independent and perfect dependent cases for each extremal symmetric dependence function V	42
511			

Table 2: $\chi(\omega)$ statistics for all stations. $\omega = 0.98, 0.985, 0.99$.

Stations	$\omega = 0.98$		$\omega = 0.985$		$\omega = 0.99$	
	$\chi(\omega)$	95% C.I.	$\chi(\omega)$	95% C.I.	$\chi(\omega)$	95% C.I.
A3472010	0.67	(-0.02, 1.00)	0.60	(-0.02, 1.00)	0.57	(-0.01, 1.00)
A4200630	0.53	(0.21, 0.81)	0.45	(0.07, 0.77)	0.38	(-0.01, 0.76)
A4250640	0.55	(0.27, 0.82)	0.49	(0.18, 0.76)	0.41	(0.02, 0.71)
A5431010	0.44	(-0.02, 1.00)	0.44	(-0.02, 1.00)	0.41	(-0.01, 1.00)
A5730610	0.59	(0.25, 0.94)	0.56	(0.20, 0.90)	0.50	(0.07, 0.97)
A6941010	0.62	(0.22, 0.99)	0.60	(0.16, 1.00)	0.56	(0.06, 1.00)
A6941015	0.63	(0.29, 0.95)	0.60	(0.20, 0.96)	0.58	(0.17, 0.98)
D0137010	0.39	(0.04, 0.69)	0.33	(-0.02, 0.67)	0.28	(-0.01, 0.69)
D0156510	0.59	(0.25, 0.88)	0.55	(0.20, 0.86)	0.53	(0.14, 0.92)
E1727510	0.62	(0.18, 0.91)	0.59	(0.16, 0.93)	0.47	(-0.01, 0.89)
E1766010	0.63	(0.23, 0.98)	0.59	(0.17, 0.96)	0.54	(0.09, 0.96)
E3511220	0.59	(0.10, 1.00)	0.53	(-0.02, 1.00)	0.50	(-0.01, 0.99)
E4035710	0.77	(0.02, 1.00)	0.68	(-0.02, 1.00)	0.60	(-0.01, 1.00)
E5400310	0.88	(0.30, 1.00)	0.89	(0.29, 1.00)	0.83	(0.13, 1.00)
E5505720	0.91	(0.24, 1.00)	0.87	(0.09, 1.00)	0.86	(0.02, 1.00)
E6470910	0.96	(0.40, 1.00)	0.94	(0.25, 1.00)	0.98	(0.00, 1.00)
H0400010	0.84	(0.12, 1.00)	0.83	(0.02, 1.00)	0.78	(-0.01, 1.00)
H1501010	0.82	(0.36, 1.00)	0.90	(0.39, 1.00)	0.84	(0.26, 1.00)
H2342010	0.68	(0.31, 1.00)	0.67	(0.25, 1.00)	0.60	(0.11, 1.00)
H5071010	0.75	(0.30, 1.00)	0.76	(0.22, 1.00)	0.75	(0.15, 1.00)
H5172010	0.80	(0.47, 1.00)	0.77	(0.42, 1.00)	0.73	(0.30, 1.00)
H6201010	0.69	(0.29, 1.00)	0.69	(0.14, 1.00)	0.69	(0.08, 1.00)
H7401010	0.85	(0.46, 1.00)	0.85	(0.38, 1.00)	0.81	(0.27, 1.00)
I9221010	0.67	(0.23, 1.00)	0.66	(0.19, 1.00)	0.59	(0.04, 1.00)
J0621610	0.61	(0.25, 0.92)	0.58	(0.20, 0.94)	0.51	(0.08, 0.91)
K0433010	0.59	(0.22, 0.91)	0.54	(0.15, 0.89)	0.45	(0.00, 0.85)
K0454010	0.71	(0.37, 1.00)	0.67	(0.24, 1.00)	0.65	(0.14, 1.00)
K0523010	0.62	(-0.02, 1.00)	0.58	(-0.02, 1.00)	0.53	(-0.01, 1.00)
K0550010	0.61	(0.22, 0.94)	0.57	(0.15, 0.94)	0.54	(0.07, 1.00)
K0673310	0.67	(0.24, 1.00)	0.65	(0.18, 1.00)	0.66	(0.07, 1.00)
K0910010	0.65	(-0.02, 1.00)	0.61	(-0.02, 1.00)	0.58	(-0.01, 1.00)
K1391810	0.68	(0.27, 1.00)	0.64	(0.16, 0.98)	0.60	(0.06, 0.96)
K1503010	0.69	(0.38, 0.98)	0.67	(0.30, 0.98)	0.64	(0.23, 1.00)
K2330810	0.68	(0.29, 1.00)	0.66	(0.22, 1.00)	0.62	(0.09, 1.00)
K2363010	0.65	(0.26, 0.98)	0.66	(0.16, 1.00)	0.61	(0.01, 1.00)
K2514010	0.61	(0.24, 1.00)	0.61	(0.21, 1.00)	0.58	(0.12, 1.00)
K2523010	0.53	(-0.02, 1.00)	0.53	(-0.02, 1.00)	0.51	(-0.01, 1.00)
K2654010	0.68	(0.37, 1.00)	0.68	(0.31, 1.00)	0.60	(0.10, 1.00)
K2674010	0.60	(0.25, 0.89)	0.58	(0.22, 0.94)	0.54	(0.08, 0.95)
K2871910	0.62	(0.26, 0.95)	0.57	(0.15, 0.94)	0.56	(0.10, 0.97)
K2884010	0.62	(0.25, 1.00)	0.57	(0.17, 0.97)	0.59	(0.16, 1.00)
K3222010	0.56	(0.21, 0.90)	0.53	(0.18, 0.93)	0.46	(0.11, 0.89)
K3292020	0.59	(0.27, 0.91)	0.57	(0.17, 0.91)	0.48	(0.07, 0.90)
K4470010	0.76	(0.39, 1.00)	0.77	(0.40, 1.00)	0.73	(0.27, 1.00)
K5090910	0.64	(0.27, 0.93)	0.64	(0.26, 0.96)	0.58	(0.12, 0.98)
K5183010	0.57	(0.14, 0.91)	0.56	(0.15, 0.96)	0.53	(0.06, 0.97)
K5200910	0.63	(0.24, 0.93)	0.62	(0.20, 0.95)	0.56	(0.11, 0.97)
L0140610	0.73	(0.23, 1.00)	0.66	(0.15, 1.00)	0.58	(-0.01, 1.00)
L0231510	0.59	(0.16, 0.91)	0.55	(0.11, 0.92)	0.53	(-0.01, 0.92)
L0400610	0.74	(-0.02, 1.00)	0.65	(-0.02, 1.00)	0.61	(-0.01, 1.00)

Table 3: Several characteristics of the Markovian estimators on Q_{50} estimation as the record length increases. Standard errors are reported in brackets.

Model	5 years			10 years			15 years			20 years	
	<i>nbias</i>	<i>var</i>	<i>nmse</i>	<i>nbias</i>	<i>var</i>	<i>nmse</i>	<i>nbias</i>	<i>var</i>	<i>nmse</i>	<i>nbias</i>	<i>var</i>
<i>log</i>	-0.35 (16e-3)	0.54 (22e-3)	0.66 (18e-3)	-0.32 (12e-3)	0.32 (12e-3)	0.42 (14e-3)	-0.30 (11e-3)	0.23 (9e-3)	0.32 (12e-3)	-0.28 (9e-3)	0.17 (7e-3)
<i>nlog</i>	-0.21 (10e-3)	0.20 (7e-3)	0.24 (11e-3)	-0.20 (7e-3)	0.11 (4e-3)	0.15 (9e-3)	-0.18 (6e-3)	0.08 (3e-3)	0.12 (8e-3)	-0.18 (5e-3)	0.06 (2e-3)
<i>mix</i>	-0.08 (8e-3)	0.14 (5e-3)	0.14 (8e-3)	-0.07 (6e-3)	0.08 (2e-3)	0.08 (6e-3)	-0.06 (5e-3)	0.05 (2e-3)	0.06 (5e-3)	-0.05 (4e-3)	0.04 (1e-3)
<i>alog</i>	-0.15 (14e-3)	0.39 (15e-3)	0.41 (14e-3)	-0.13 (10e-3)	0.22 (9e-3)	0.24 (11e-3)	-0.11 (9e-3)	0.16 (6e-3)	0.17 (9e-3)	-0.10 (8e-3)	0.12 (4e-3)
<i>anlog</i>	-0.10 (10e-3)	0.20 (7e-3)	0.21 (10e-3)	-0.09 (7e-3)	0.11 (4e-3)	0.12 (8e-3)	-0.08 (6e-3)	0.08 (2e-3)	0.09 (6e-3)	-0.08 (5e-3)	0.06 (2e-3)
<i>amix</i>	-0.06 (7e-3)	0.11 (4e-3)	0.12 (7e-3)	-0.05 (6e-3)	0.06 (2e-3)	0.06 (6e-3)	-0.04 (5e-3)	0.04 (1e-3)	0.05 (5e-3)	-0.03 (4e-3)	0.03 (1e-3)

Table 4: Several characteristics of the *amix*, *MLE*, *PWU* and *PWB* estimators for Q_{50} estimation as the record length increases. Standard errors are reported in brackets.

Model	5 years			10 years			15 years			20 years		
	<i>nbias</i>	<i>var</i>	<i>nmse</i>	<i>nbias</i>	<i>var</i>	<i>nmse</i>	<i>nbias</i>	<i>var</i>	<i>nmse</i>	<i>nbias</i>	<i>var</i>	<i>nmse</i>
<i>amix</i>	-0.06 (8e-3)	0.11 (4e-3)	0.12 (8e-3)	-0.05 (6e-3)	0.06 (2e-3)	0.07 (6e-3)	-0.04 (5e-3)	0.04 (1e-3)	0.05 (5e-3)	-0.04 (4e-3)	0.03 (1e-3)	0.04 (4e-3)
<i>MLE</i>	-0.13 (12e-3)	0.25 (15e-3)	0.27 (12e-3)	-0.14 (8e-3)	0.13 (6e-3)	0.14 (9e-3)	-0.13 (7e-3)	0.08 (3e-3)	0.10 (7e-3)	-0.11 (5e-3)	0.05 (2e-3)	0.06 (6e-3)
<i>PWU</i>	0.08 (13e-3)	0.30 (13e-3)	0.31 (13e-3)	-0.01 (9e-3)	0.15 (6e-3)	0.15 (9e-3)	-0.03 (7e-3)	0.10 (3e-3)	0.10 (7e-3)	-0.03 (6e-3)	0.06 (2e-3)	0.07 (6e-3)
<i>PWB</i>	-0.07 (10e-3)	0.20 (8e-3)	0.21 (11e-3)	-0.10 (7e-3)	0.11 (4e-3)	0.12 (8e-3)	-0.11 (6e-3)	0.08 (2e-3)	0.09 (7e-3)	-0.10 (5e-3)	0.05 (1e-3)	0.06 (6e-3)

Table 5: Partial and mixed partial derivatives, definition domain, total independent and perfect dependent cases for each extremal symmetric dependence function V .

Model	Symmetric Models		
	<i>log</i>	<i>nlog</i>	<i>mix</i>
$V(x, y)$	$(x^{-1/\alpha} + y^{-1/\alpha})^\alpha$	$\frac{1}{x} + \frac{1}{y} - (x^\alpha + y^\alpha)^{-1/\alpha}$	$\frac{1}{x} + \frac{1}{y} - \frac{\alpha}{x+y}$
$V_1(x, y)$	$-x^{-\frac{1}{\alpha}-1}V(x, y)^{\frac{\alpha-1}{\alpha}}$	$-\frac{1}{x^2} + x^{\alpha-1}(x^\alpha + y^\alpha)^{-\frac{1}{\alpha}-1}$	$-\frac{1}{x^2} + \frac{\alpha}{(x+y)^2}$
$V_2(x, y)$	$-y^{-\frac{1}{\alpha}-1}V(x, y)^{\frac{\alpha-1}{\alpha}}$	$-\frac{1}{y^2} + y^{\alpha-1}(x^\alpha + y^\alpha)^{-\frac{1}{\alpha}-1}$	$-\frac{1}{y^2} + \frac{\alpha}{(x+y)^2}$
$V_{12}(x, y)$	$-(xy)^{-\frac{1}{\alpha}-1}\frac{1-\alpha}{\alpha}V(x, y)^{\frac{\alpha-2}{\alpha}}$	$-(\alpha+1)(xy)^{\alpha-1}(x^\alpha + y^\alpha)^{-\frac{1}{\alpha}-2}$	$-\frac{2\alpha}{(x+y)^3}$
$A(w)$	$\left[(1-w)^{\frac{1}{\alpha}} + w^{\frac{1}{\alpha}}\right]^\alpha$	$1 - [(1-w)^{-\alpha} + w^{-\alpha}]^{-\frac{1}{\alpha}}$	$1 - w(1-w)\alpha$
Independence	$\alpha = 1$	$\alpha \rightarrow 0$	$\alpha = 0$
Total dependence	$\alpha \rightarrow 0$	$\alpha \rightarrow +\infty$	Never reached
Constraint	$0 < \alpha \leq 1$	$\alpha > 0$	$0 \leq \alpha \leq 1$